Acta Crystallographica Section D
Biological Crystallography
ISSN 0907-4449

Sweet neutron crystallography

S. C. M. Teixeira,[a,b]* M. P. Blakeley,[b] R. M. F. Leal,[c] S. M. Gillespie,[a,b] E. P. Mitchell[c] and V. T. Forsyth[a,b]

[a]EPSAM, Keele University, Keele, Staffordshire ST5 5BG, England, [b]Institut Laue–Langevin, 6 Rue Jules Horowitz, 38042 Grenoble CEDEX 9, France, and [c]ESRF, 6 Rue Jules Horowitz, BP 220, 38043 Grenoble, France

Correspondence e-mail: s.c.m.teixeira@natsci.keele.ac.uk

Received 30 April 2010
Accepted 26 May 2010

Extremely sweet proteins isolated from tropical fruit extracts are promising healthy alternatives to sugar and synthetic sweeteners. Sweetness and taste in general are, however, still poorly understood. The engineering of stable sweet proteins with tailored properties is made difficult by the lack of supporting high-resolution structural data. Experimental information on charge distribution, protonation states and solvent structure are vital for an understanding of the mechanism through which sweet proteins interact with taste receptors. Neutron studies of the crystal structures of sweet proteins allow a detailed study of these biophysical properties, as illustrated by a neutron study on the native protein thaumatin in which deuterium labelling was used to improve data quality.

1. Introduction

The perception of sweet and bitter taste plays an essential role in human life. Our environment and habits have changed dramatically from those of our primate ancestors, yet we are still hardwired to seek food with high energetic content. The exponential growth in the number of people suffering from obesity, diabetes and a number of diseases related to the consumption of sugar is a major health concern. Biotechnologists face a major challenge to engineer healthier, stable sweeteners that can be used in food, drinks and pharmaceutical applications.

In humans, as in many animals, specific membrane proteins in the taste buds in the mouth are responsible for sensing ligands and triggering an intracellular pathway that ultimately translates into the detection of odours and flavours, as well as the tastes salty, sour, sweet, bitter and umami (also known as savoury; Mombaerts, 2004). Taste is a fascinatingly complex sense and its mechanisms remain elusive despite being pursued by many researchers: sweet and umami taste receptors (G-protein-coupled receptors or GPCRs) were discovered in 2001 (see, for example, Li *et al.*, 2002; Zhao *et al.*, 2003), but their structures have yet to be determined.

The current proposed structure for the human sweet taste receptor (Nelson *et al.*, 2001; Tsuchiya *et al.*, 2002), a GPCR heterodimer (hT1R2–T1R3), assumes homology to a glutamate receptor (Mombaerts, 2001); the active site was modelled according to shape and charge complementarity to rigid small-molecule sweeteners (Temussi *et al.*, 1991; Cui *et al.*, 2006). For proteins, the so-called wedge model of interaction with hT1R2–T1R3 has been proposed (Temussi, 2002): it postulates

a large multi-point surface of interaction between the protein and the receptor, as opposed to small sweeteners (such as aspartame and saccharin) which activate the receptor through point specific interactions. This is consistent with findings that regions remote from each other within the structures of sweet proteins play roles in the modulation of sweetness (Assadi-Porter *et al.*, 2000; Chen *et al.*, 2008; Spadaccini *et al.*, 2003).

1.1. Sweet proteins and thaumatin

A number of tropical plant proteins have been found to be potent sweeteners (de Vos *et al.*, 1985), such as thaumatin (van der Wel & Loeve, 1972; Faus *et al.*, 1996) and monellin (Inglett & May, 1969). Their biological role in plants is not well understood, although it is known that they are produced as a response to biotic (fungal pathogens; Ruiz-Medrano *et al.*, 1992) or abiotic stress. Monomeric thaumatin is an intensely sweet protein (for some applications it is 3000 times sweeter than sucrose on a weight basis; Boy, 2010) that is currently used as a sweetener, taste modifier and enhancer (for example, as a masking agent in medicines and cigarettes; Gibbs *et al.*, 1996).

Thaumatin can lower the threshold for savoury-flavour compounds and acts as a flavour enhancer below the sweetness threshold. At neutral pH, it becomes unstable at temperatures above 343 K and loses sweetness (Kaneko & Kitabatake, 1999). Thaumatin can also have a lingering 'liquorice' aftertaste at high usage levels.

There are at least five intensely sweet forms of thaumatin. The two most abundant components, thaumatin I and II, differ by only five out of 207 amino acids. The sequence of thaumatin is characteristic of a family of pathogenesis-related proteins (PR5; Selitrennikoff, 2001) produced in plants as a response to infection. However, PR5s are not sweet, even when they have a thaumatin-like tertiary structure (Somoza *et al.*, 1993). On the other hand, no common structural basis has so far been identified between thaumatin and other sweet proteins, except for their basicity (thaumatin remains positively charged up to pH 12). The presence and distribution of positively charged residues has been postulated to play a role in sweetness, namely the presence of lysine residues surrounding a cleft region in the structure of thaumatin (Kaneko & Kitabatake, 2001*a*), but mutation studies have shown that it is not in itself the determining factor.

Thaumatin is a protein well known to X-ray crystallographers: protocols to grow relatively large crystals (typically volumes of 0.1 mm^3) have been well established (see, for example, Barnes *et al.*, 2002). High-resolution X-ray crystal structures of thaumatin (the highest resolution at present is 0.94 Å; Asherie *et al.*, 2009) have been determined at different temperatures and pH values. None of these include information on the positions of H atoms or the orientations of water molecules. Inferred positions of H atoms (*i.e.* from the chemical context of the structure), which are often carried out by necessity owing to the lack of sensitivity of most structural techniques to hydrogen in biomacromolecules, can be particularly misleading. The local chemical environment within a structure (*e.g.* Lo Leggio *et al.*, 2001; Seyedarabi *et al.*, 2010) often leads to dramatic deviations from theoretical pK_a values. Neutron crystallography is the technique of choice to directly determine all protonation states, charge distribution and solvent structure.

1.2. Neutron crystallography

At the Institut Laue–Langevin (ILL), neutron crystallographic studies of biological macromolecules (Teixeira, Ankner *et al.*, 2008; Leal *et al.*, 2009) benefit from a world-leading suite of three instruments: LADI, a high-resolution diffractometer that uses a quasi-Laue technique ($2.6 < \lambda < 4.5$ Å), D19, a monochromatic instrument that uses thermal neutrons ($0.8 < \lambda < 2.4$ Å), and a low-resolution monochromatic diffractometer for large macromolecular complexes, D16 ($4.5 < \lambda < 7.56$ Å). For high-resolution studies, LADI is a highly effective instrument where crystal samples can have larger unit-cell edges (150 Å on an edge; Blakeley *et al.*, 2008) and relatively small crystals can be used (typically 0.1 mm^3 if perdeuterated). The D19 diffractometer (Kovalevsky *et al.*, 2010; Forsyth *et al.*, 1998) can record data to higher resolution than LADI, but is limited to smaller unit cells and typically requires crystal volumes of 1 mm^3 or greater.

Both the LADI and D19 instruments are suitable for neutron crystallographic studies of thaumatin: preliminary work on LADI (Teixeira, Ankner *et al.*, 2008) and a recent test on D19 (data not shown) have demonstrated the scope of each instrument. Both the LADI and D19 tests were carried out using hydrogenated protein in heavy-water buffers. This allows the exchangeable H atoms to be replaced by deuterium and helps minimize the incoherent scattering background.

2. Materials and methods

2.1. Sample preparation

Lyophilized thaumatin from *Thaumatococcus daniellii* (Sigma–Aldrich) was dissolved in heavy water, centrifuged at 12 000 rev min^{-1} and filtered (0.22 µm pore Millipore filter). The crystallization buffer used (pD 6.5) was prepared with heavy water, using L-tartrate as the precipitating agent. Bipyramidal thaumatin crystals were grown directly in quartz capillaries at 293 K as described previously (Teixeira, Blakeley *et al.*, 2008).

2.2. Diffraction data collection

Neutron quasi-Laue data were collected at room temperature on the LADI-III beamline installed on cold neutron guide H142 at the Institut Laue–Langevin. Using a crystal of volume 1.4 mm^3, diffraction spots were observed up to 1.8 Å resolution. Data were subsequently processed to 2.1 Å. As is typical for a Laue experiment, the crystal was held stationary at a different φ setting for each 12 h exposure. Three crystal orientations were used such that the complete data set comprised 21 images covering 49° of data in angular steps of 7°, 45° of data in angular steps of 5° and finally 35° of data in angular steps of 7°. The neutron Laue data images were

Table 1
Crystallographic data collected from a sample of native thaumatin grown in a deuterated crystallization buffer.

Values in parentheses are for the highest resolution shell.

	X-ray data	Neutron data
Wavelength (Å)	1.54	3.25–4.20
Resolution (Å)	19.59–1.90 (2.00–1.90)	57.83–2.10 (2.21–2.10)
Mean $I/\sigma(I)$	41.20 (12.76)	11.80 (1.70)
Completeness	98.50 (90.30)	71.70 (51.30)
$R_{\rm merge}$† (%)	2.90 (16.30)	13.60 (25.20)
$R_{\rm meas}$‡ (%)	7.00 (36.50)	14.60 (28.20)
Multiplicity	26.10 (18.99)	5.60 (3.40)
Total reflections	538215 (49833)	10809 (1096)
Unique reflections	20585 (2624)	1930 (322)

† $R_{\rm merge} = \sum_{hkl}\sum_i |I_i(hkl) - \langle I(hkl)\rangle| / \sum_{hkl}\sum_i I_i(hkl)$. ‡ $R_{\rm meas} = \sum_{hkl}[N/(N-1)]^{1/2} \times \sum_i |I_i(hkl) - \langle I(hkl)\rangle| / \sum_{hkl}\sum_i I_i(hkl)$, where $I_i(hkl)$ is the intensity of the ith observation of reflection (hkl) and N is the redundancy.

processed using the Daresbury Laboratory *LAUE* suite program *LAUEGEN* in a version modified to account for the cylindrical geometry of the detector (Campbell *et al.*, 1998). The program *LSCALE* (Arzt *et al.*, 1999) was used to determine the wavelength-normalization curve using the intensities of symmetry-equivalent reflections measured at different wavelengths and to apply wavelength-normalization calculations to the observed data. The data were then scaled and merged in *SCALA* (Collaborative Computational Project, Number 4, 1994). Data-reduction statistics are shown in Table 1.

Room-temperature X-ray data were also collected from the same crystal sample using an in-house rotating-anode generator source and a MAR 345 diffractometer. X-ray data were processed with the *XDS* program package (Kabsch, 2010). Diffraction data were indexed in space group $P4_12_12$, with unit-cell parameters $a = b = 57.81$, $c = 150.02$ Å. The crystal solvent content was 54% (calculated Matthews coefficient of 2.68 Å^3 Da^{-1}; Matthews, 1968).

2.3. Structure analysis

The structures shown in Fig. 2 were selected from the PDB (Berman *et al.*, 2003): the highest resolution structure available was taken as a representative for each space group. The program *DSSP* was used to define the secondary structure (Kabsch & Sander, 1983). Structural alignments of protein backbone atoms were performed using the program *SUPERPOSE* (Krissinel & Henrick, 2004), with the tetragonal crystal structure as a reference (PDB code 2vhk; Asherie *et al.*, 2009). Root-mean-square deviation (r.m.s.d.) values were within ∼0.3–0.7 Å. Images were prepared with the program *PyMOL* (DeLano, 2002).

3. Results and discussion

3.1. The use of partially deuterated proteins

Crystals of thaumatin have relatively large unit cells for neutron studies (see, for example, Blakeley, 2009), providing a good measure of the feasibility of using neutron crystallography to study sweet proteins of similar or smaller sizes while providing information on solvent accessibility, protonation states and water-molecule orientations.

The samples used for the studies described here were partially deuterated by virtue of crystallization in solutions prepared with D_2O. Neutron crystallographic data provide nuclear density maps in which moderately well ordered residues such as glutamic acid and glutamine, for example, which are typically difficult to discriminate without high-resolution X-ray data, clearly differ (see Fig. 1). The strong coherent neutron scattering contribution from deuterium (compared with hydrogen) resolves ambiguities between the neutron scattering density maps of amine and carboxyl groups. For the case of thaumatin this is particularly interesting, as thaumatin I and II differ by only five amino acids and can form heterogeneous crystals for which the corresponding structural models average the mixture present in the crystalline lattice (see, for example, the structure with PDB code 1rqw; Q. Ma & G. M. Sheldrick, unpublished work). Complementary information is also available from the extent of exchange of hydrogen to deuterium. The occupancies of the exchangeable H atoms in the structure are a function of solvent accessibility and hydrogen-bond stability, reflecting information that is directly relevant to the interaction between sweet proteins and receptors.

3.2. Solvent structure and electrostatic distribution

Owing to a combination of factors associated with neutron Laue data collection from partially deuterated crystals of large

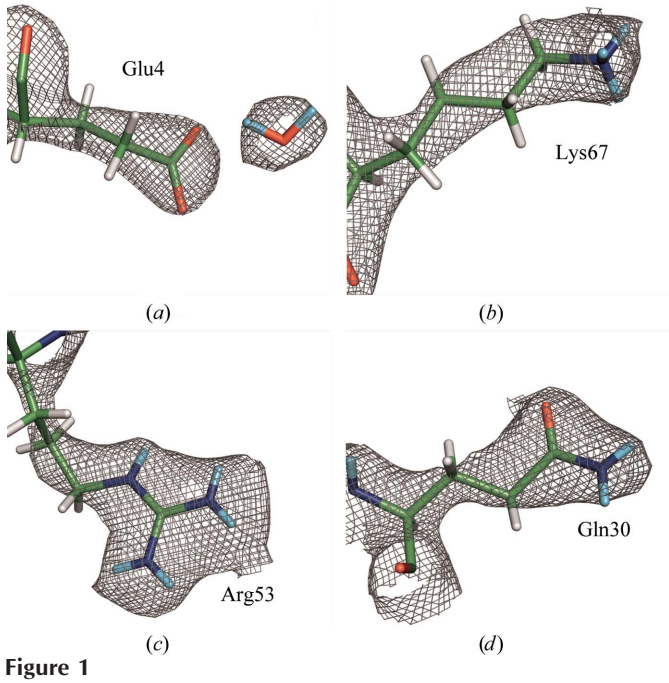

Figure 1
Neutron scattering density map of the native thaumatin crystal structure (see preliminary study; Teixeira, Blakeley *et al.*, 2008), represented at the 1σ level, for the side chains of the amino acids (*a*) glutamate 4, where an oriented water molecule is also shown, (*b*) lysine 67, (*c*) arginine 53 and (*d*) glutamine 30. The structure is represented as sticks coloured by element type; carbon in green, nitrogen in blue, deuterium in cyan, hydrogen in white and oxygen in red.

unit-cell systems on a fixed-radius cylindrical detector such as LADI-III (*e.g.* spatial overlap of reflections and a large blind region), neutron Laue data sets typically have a lower completeness than monochromatic X-ray diffraction data sets (Gardberg *et al.*, 2010). The joint use of X-ray and neutron data to refine structural models is therefore a very positive approach that not only extends the experimental data but also provides an independent cross-check between density maps that validates the final structure. Future work will involve a joint neutron/X-ray structure refinement to determine H/D-atom positions, particularly those in the typically charged residues that are central to the potential electrostatic interaction of thaumatin with other molecules. It has been observed previously that these residues are not randomly distributed across thaumatin structures (Charron *et al.*, 2004) and the same is true for other sweet proteins, although a sweetness-related trend has not been proven.

Evidence for the role of charge and electrostatic distribution in thaumatin comes from its observed masking effects on the bitter taste of metallic positive ions such as sodium, while it enhances that of negative ions such as chloride (Natex UK Ltd, 2010). However, Fig. 2(*a*) shows no major structural changes in representative structures observed under different crystallization conditions. The crystal structures shown in Fig. 2(*a*) correspond to cryocooled samples obtained at a range of temperatures, pH values (from pH 4.5 in the hexagonal lattice to pH 8 in the orthorhombic form) and in the presence of different salts and buffers. The variety of conditions and the lack of high-resolution data at room temperature makes it difficult to detect trends, particularly those buried under very similar secondary structures and folds, but Fig. 2(*a*) shows clear differences in the loop regions of the structures of thaumatin crystallized in different space groups. Similar loop regions were believed in the past to act as 'sweet fingers' (Spadaccini *et al.*, 2001) that could activate different point interaction sites of the receptor through a mechanism similar to small-molecule sweeteners.

It has been shown previously that the thermoinactivation (loss of sweetness) and thermostability of thaumatin are very dependent on pH (Kaneko & Kitabatake, 2001*b*). However, the nondestructive nature of neutron radiation to crystals of biomacromolecules allows structures to be determined at the same temperature at which the crystals were formed, eliminating ambiguities introduced by cryocooling and allowing deeper dynamic and structural insights (Weik & Colletier, 2010). Furthermore, the same crystal sample can be used for X-ray diffraction studies at room temperature (benefiting in this case from the large crystal size and the relative resistance of thaumatin to X-ray radiation damage; Borek *et al.*, 2010).

The so-called 'biological water' structure of other sweet proteins such as monellin (the layer of water either directly bound to the protein or involved in solvation of ions) has already been a subject of studies into the role of solvation and protein flexibility, both of which are central to the structure–activity relationship (Hobbs *et al.*, 2007; Hansia *et al.*, 2006). Tightly bound waters that are not present in a less sweet mutant of monellin (De Simone *et al.*, 2006) have been suggested to be implicated in decreasing the accessibility of the protein surface to interactions with the receptor. Fig. 2(*b*) shows that water molecules that are conserved across thaumatin structures in different space groups do have a non-random distribution of lower temperature factors, hinting at a tighter binding of water to the α-helical region of the secondary structure. Future studies will provide a detailed and accurate description of the solvent structure of thaumatin. The use of perdeuterated samples will be a major advantage when used for neutron crystallography, as it not only allows easier identification of water structure, and distinction from sodium or potassium ions for example, but will also allow the orientation of the molecules to be defined.

A new approach to structure–activity relationship studies is extremely timely and neutron diffraction can provide an important contribution towards understanding the structural basis of the sweetness of thaumatin and other natural proteins.

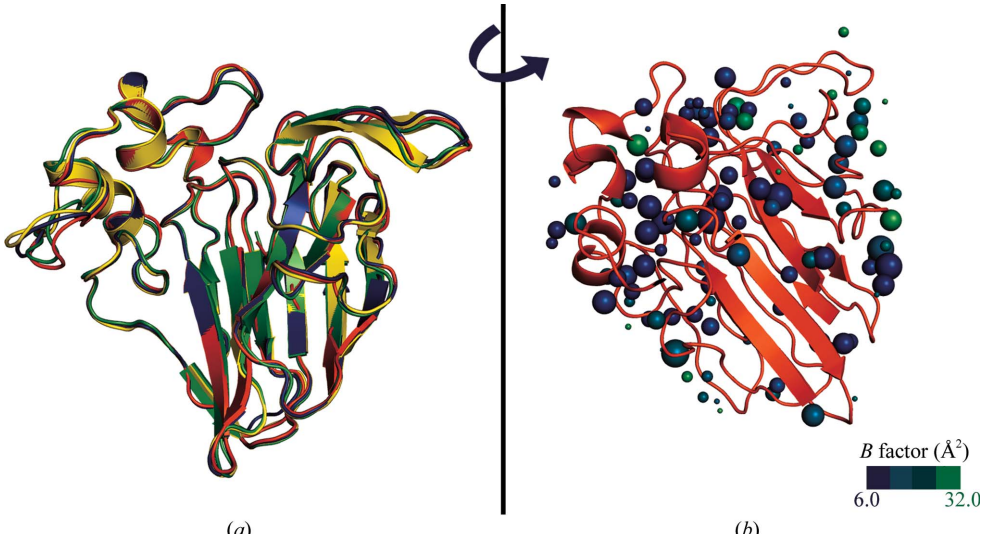

Figure 2
A comparison of different thaumatin structures. (*a*) A superposition of thaumatin structures determined in different space groups. The maximum root-mean-square difference is 0.636 Å and is observed in the loop regions of the structure. The colour code highlights different crystal systems: tetragonal in red (PDB code 2vhk; Asherie *et al.*, 2009), hexagonal in yellow (PDB code 1pp3; Charron *et al.*, 2004), orthorhombic in blue (PDB code 2vu6; Asherie *et al.*, 2009) and monoclinic in green (PDB code 1thu; Ko *et al.*, 1994). (*b*) Water molecules conserved across different space groups are highlighted (for clarity, only the tetragonal structure is shown, in red). Water molecules are displayed as spheres coloured according to *B* factor as shown in the spectrum bar, with radii proportional to their conservation (only waters within 0.7 Å, which is the maximum r.m.s.d. observed for the aligned structures, were taken as conserved; the sphere radii are largest for waters within 0.15 Å of each other).

SCMT would like to acknowledge useful discussions with Dr Charles Boy, Natex UK Ltd as well as with the Deuteration Laboratory staff. SMG would like to acknowledge studentship support from Keele University and the Engineering and Physical Sciences Research Council (EPSRC). VTF acknowledges the EPSRC for support under grants GR/R47950/01, GR/R99393/01 and EP/C015452/1. This work has also benefited from activities associated with EU project funding under contracts 226507-NMI3, STRP-033256 and RII3-CT-2003-505925. We acknowledge the ILL for beam time.

References

Arzt, S., Campbell, J. W., Harding, M. M., Hao, Q. & Helliwell, J. R. (1999). *J. Appl. Cryst.* **32**, 554–562.
Asherie, N., Jakoncic, J., Ginsberg, C., Greenbaum, A., Stojanoff, V., Hrnjez, B. J., Blass, S. & Berger, J. (2009). *Cryst. Growth Des.* **9**, 4189–4198.
Assadi-Porter, F. M., Aceti, D. J. & Markley, J. L. (2000). *Arch. Biochem. Biophys.* **376**, 259–265.
Barnes, C. L., Snell, E. H. & Kundrot, C. E. (2002). *Acta Cryst.* D**58**, 751–760.
Berman, H. M., Henrick, K. & Nakamura, H. (2003). *Nature Struct. Biol.* **10**, 980.
Blakeley, M. P. (2009). *Crystallogr. Rev.* **15**, 157–218.
Blakeley, M. P., Langan, P., Niimura, N. & Podjarny, A. (2008). *Curr. Opin. Struct. Biol.* **18**, 593–600.
Borek, D., Cymborowski, M., Machius, M., Minor, W. & Otwinowski, Z. (2010). *Acta Cryst.* D**66**, 426–436.
Boy, C. (2010). Personal communication.
Campbell, J. W., Hao, Q., Harding, M. M., Nguti, N. D. & Wilkinson, C. (1998). *J. Appl. Cryst.* **31**, 496–502.
Charron, C., Giegé, R. & Lorber, B. (2004). *Acta Cryst.* D**60**, 83–89.
Chen, C.-C., Wei, C.-C., Sun, Y.-C. & Chen, C.-M. (2008). *J. Struct. Biol.* **162**, 237–247.
Collaborative Computational Project, Number 4 (1994). *Acta Cryst.* D**50**, 760–763.
Cui, M., Jiang, P., Maillet, E., Max, M., Margolskee, R. F. & Osman, R. (2006). *Curr. Pharm. Des.* **12**, 4591-4600.
DeLano, W. L. (2002). *PyMOL.* DeLano Scientific, San Carlos, California, USA. http://www.pymol.org.
De Simone, A., Spadaccini, R., Temussi, P. A. & Fraternali, F. (2006). *Biophys. J.* **90**, 3052–3061.
De Vos, A. M., Hatada, M., van der Wel, H., Krabbendam, H., Peerdeman, A. F. & Kim, S.-H. (1985). *Proc. Natl Acad. Sci. USA*, **82**, 1406–1409.
Faus, I., Patino, C., Rio, J. L., del Moral, C., Barroso, H. S. & Rubio, V. (1996). *Biochem. Biophys. Res. Commun.* **229**, 121–127.
Forsyth, V. T., Shotton, M. W., Ye, H., Boote, C., Langan, P., Pope, L. H. & Denny, R. C. (1998). *Fibre Diffraction Rev.* **7**, 17–24.
Gardberg, A. S., Del Castillo, A. R., Weiss, K. L., Meilleur, F., Blakeley, M. P. & Myles, D. A. A. (2010). *Acta Cryst.* D**66**, 558–567.
Gibbs, B. F., Alli, I. & Mulligan, C. (1996). *Nutr. Res.* **16**, 1619–1630.
Hansia, P., Vishveshwara, S. & Pal, S. K. (2006). *Chem. Phys. Lett.* **420**, 512–517.
Hobbs, J. R., Munger, S. D. & Conn, G. L. (2007). *Acta Cryst.* F**63**, 162–167.
Inglett, G. E. & May, J. F. (1969). *J. Food Sci.* **34**, 408–411.
Kabsch, W. (2010). *Acta Cryst.* D**66**, 125–132.
Kabsch, W. & Sander, C. (1983). *Biopolymers*, **22**, 2577–2637.
Kaneko, R. & Kitabatake, N. (1999). *J. Agric. Food Chem.* **47**, 4950–4955.
Kaneko, R. & Kitabatake, N. (2001*a*). *Chem. Senses*, **26**, 167–177.
Kaneko, R. & Kitabatake, N. (2001*b*). *Biosci. Biotechnol. Biochem.* **65**, 409–413.
Ko, T.-P., Day, J., Greenwood, A. & McPherson, A. (1994). *Acta Cryst.* D**50**, 813–825.
Kovalevsky, A. Y., Hanson, L., Fisher, S. Z., Mustyakimov, M., Mason, S. A., Forsyth, V. T., Blakeley, M. P., Keen, D., Wagner, T., Carrell, H. L., Katz, A. K., Glusker, J. P. & Langan, P. (2010). *Structure*, **18**, 688–699.
Krissinel, E. & Henrick, K. (2004). *Acta Cryst.* D**60**, 2256–2268.
Leal, R. M. F., Teixeira, S. C. M., Blakeley, M. P., Mitchell, E. P. & Forsyth, V. T. (2009). *Acta Cryst.* F**65**, 232–235.
Li, X., Staszewski, X., Xu, H., Durick, K., Zoller, M. & Adler, E. (2002). *Proc. Natl Acad. Sci. USA*, **99**, 4692–4694.
Lo Leggio, L., Kalogiannis, S., Eckert, K., Teixeira, S. C., Bhat, M. K., Andrei, C., Pickersgill, R. W. & Larsen, S. (2001). *FEBS Lett.* **509**, 303–308.
Matthews, B. W. (1968). *J. Mol. Biol.* **33**, 491–497.
Mombaerts, P. (2001). *Annu. Rev. Genomics Hum. Genet.* **2**, 463–492.
Mombaerts, P. (2004). *Nature Rev. Neurosci.* **5**, 263–278.
Natex UK Ltd (2010). *Thaumatin from Natex UK Limited.* http://www.natexuk.com.
Nelson, G., Hoon, M. A., Chandrashekar, J., Zhang, Y., Ryba, N. J. & Zuker, C. S. (2001). *Cell*, **106**, 381–390.
Ruiz-Medrano, R., Jimenez-Moraila, B., Herrera-Estrella, L. & Rivera-Bustamante, R. F. (1992). *Plant Mol. Biol.* **20**, 1199–1202.
Selitrennikoff, C. P. (2001). *Appl. Environ. Microb.* **67**, 2883–2894.
Seyedarabi, A., To, T. T., Ali, S., Hussain, S., Fries, M., Madsen, R., Clausen, M. H., Teixteira, S., Brocklehurst, K. & Pickersgill, R. W. (2010). *Biochemistry*, **49**, 539–546.
Somoza, J. R., Jiang, F., Tong, L., Kang, C.-H., Cho, J. M. & Kim, S.-H. (1993). *J. Mol. Biol.* **234**, 390–404.
Spadaccini, R., Crescenzi, O., Tancredi, T., De Casamassimi, N., Saviano, G., Scognamiglio, R., Di Donato, A. & Temussi, P. A. (2001). *J. Mol. Biol.* **305**, 505–514.
Spadaccini, R., Trabucco, F., Saviano, G., Picone, D., Crescenzi, O., Tancredi, T. & Temussi, P. A. (2003). *J. Mol. Biol.* **328**, 683–692.
Teixeira, S. C. M., Ankner, J. *et al.* (2008). *Chem. Phys.* **345**, 133–151.
Teixeira, S. C. M., Blakeley, M. P., Leal, R. M. F., Mitchell, E. P. & Forsyth, V. T. (2008). *Acta Cryst.* F**64**, 378–381.
Temussi, P. A., Lelj, F. & Tancredi, T. (1991). *ACS Symp. Ser.* **450**, 143–161.
Temussi, P. A. (2002). *FEBS Lett.* **526**, 1–4.
Tsuchiya, D., Kunishima, N., Kamiya, N., Jingami, H. & Morikawa, K. (2002). *Proc. Natl Acad. Sci. USA*, **99**, 4692–4696.
Weik, M. & Colletier, J.-P. (2010). *Acta Cryst.* D**66**, 437–446.
Wel, H. van der & Loeve, K. (1972). *Eur. J. Biochem.* **31**, 221–225.
Zhao, G., Zhang, Y., Hoon, M., Chandrashekar, J., Erlenbach, I., Ryba, N. & Zuker, C. (2003). *Cell*, **115**, 255–266.